

## Energy Dependence of Fission Fragment Anisotropy\*†

JAMES J. GRIFFIN

*Los Alamos Scientific Laboratory, University of California, Los Alamos, New Mexico*

(Received April 7, 1958; revised manuscript received May 25, 1959)

The dependence on energy of the anisotropy of fission fragment emission is discussed in terms of the Bohr model. It is shown that reasonable assumptions about the spectrum of excited states at the barrier lead to results consistent with the currently available data for energies up to 10 Mev and for a variety of target nuclides, except for the fact that the target spin appears to have a much smaller effect on the anisotropy than might have been predicted. It is suggested that this anomaly may be understood in terms of the deformation of the target nucleus.

### I. INTRODUCTION

SOME implications of Bohr's theory of fission fragment anisotropy<sup>1</sup> are analyzed especially as regards energy dependence. Section II summarizes some of the ideas of Bohr and their application to anisotropy in photofission and neutron-induced fission, and outlines the general qualitative features of the dependence of anisotropy on energy.

It is shown that one must expect the anisotropy to increase at the energy where each new ( $n, xn'f$ ) process becomes energetically possible and to decrease until the next threshold is reached. The amplitude of such increases will depend chiefly on the proportion of ( $n, xn'f$ ) processes relative to the total number of fissions. The effect on anisotropy of the staggering of the difference between the fission threshold and the neutron binding energy from even-even to even-odd nuclides is discussed. In Sec. III, parameters inferred from the anisotropy of Pu<sup>239</sup> fission are shown to give a satisfactory account of the anisotropy of U<sup>235</sup>, U<sup>238</sup>, and Th<sup>232</sup>. These estimates involve various approximations and are not to be considered precise. Still, they establish the fact that reasonable assumptions about the barrier spectrum are capable of yielding theoretical anisotropies in agreement with the currently available data. In Sec. IV, the results are discussed and the conclusion drawn that the theory does give a reasonably good description of the experimental facts, apart from the expected, but unobserved, effect of target spin.

### II. FISSION AND THE EXCITATION SPECTRUM AT THE BARRIER

Bohr<sup>1</sup> has discussed the anisotropy observed in fission fragment emission in terms of the excitation spectrum at the fission barrier. He points out that for excitation energies  $E^*$  only slightly in excess of the lowest fission barrier energy  $E_F$ , the nucleus at the barrier is "cold," having expended most of its available energy in potential energy of deformation in reaching

the barrier. Since a nucleus at the barrier is strongly deformed, its spectrum should resemble those of stably deformed nuclei at an excitation energy  $E_{exc} = E^* - E_F$ . The assumed "spectrum" at the barrier is at best quasi-stationary, and, in fact, the notion of such a spectrum is an accurate one only if the nucleus remains at the barrier for a time long compared with the periods of the excitations in question. However, Strutinskii<sup>2</sup> has shown that an expression of the same form as that obtained by Bohr may be derived without the explicit assumption that the spectrum is quasi-stationary.

Bohr assumes that the nucleus retains axial symmetry throughout the fission process, and that the fragments are emitted in the direction of the nuclear symmetry axis. The distribution of orientations of the symmetry axis then gives the angular distribution of the fragments. For a compound state of angular momentum  $I$ , and  $Z$  component (along the beam)  $M$ , which traverses the barrier in a state of intrinsic excitation with component  $K$  of angular momentum along the symmetry axis, the distribution is given simply by the square of the symmetric top wave function:

$$W(\theta) \propto |D_{MK}^I(\theta)|^2. \quad (1)$$

#### 1. Photofission of Even-Even Targets

##### (a) Dipole

The photofission of even-even nuclei (which have spin zero) is an especially simple case to analyze in these terms. If the photon is absorbed in the electric dipole mode, the compound state has  $I=1$ ,  $M=\pm 1$ . Moreover, in an even-even nucleus, low-lying states are characterized by the pairing of nucleons to states with  $K=0$ . More specifically, low-lying  $1^-$  states with  $K=0$  have been observed in the spectra of deformed nuclei,<sup>3</sup> and have been associated with a collective asymmetric shape vibration.<sup>1,4-6</sup> For photofission through such a

<sup>2</sup> V. M. Strutinskii, J. Exptl. Theoret. Phys. (U.S.S.R.) **30**, 606 (1956) [translation: Soviet Phys. JETP **3**, 638 (1956)].

<sup>3</sup> Stephens, Asaro, and Perlman, Phys. Rev. **96**, 1568 (1954); **100**, 1543 (1955).

<sup>4</sup> V. M. Strutinskii, Atomnaya Energy **4**, 611 (1956) [translation: Soviet J. Atomic Energy **4**, 150 (1956)].

<sup>5</sup> D. R. Inglis, Phys. Rev. **108**, 774 (1957).

<sup>6</sup> L. Wilets and J. Griffin (to be published).

\* Work performed under the auspices of the U. S. Atomic Energy Commission.

† Present address: Department of Mathematical Physics, University of Birmingham, England.

<sup>1</sup> A. Bohr, *Proceedings of the International Conference on the Peaceful Uses of Atomic Energy, Geneva, 1955* (United Nations, New York, 1956), Vol. 2, p. 151.

state at the barrier, the angular distribution would be

$$W(\theta) \propto |D_{\pm 1, 0}^1|^2 \propto \sin^2\theta. \quad (2)$$

In this way Bohr can explain the observed<sup>7,8</sup> emission of fragments in the direction  $90^\circ$  from the beam.

(b) *Quadrupole*

For quadrupole absorption of the photon, the compound state will have quantum numbers  $I=2$ ,  $M=\pm 1$ , and the lowest corresponding excitation at the barrier would be a  $2^+$  state with  $K=0$ , the second member of the even parity rotational band. If at the barrier, this state lies sufficiently low compared with the  $1^-$  state, then there might exist a range of photon energies over which the smaller probability of quadrupole absorption is counterbalanced by the smaller probability of fission through the  $1^-$  state. The resulting angular distribution of fission fragments would have a component of the form

$$W(\theta) \propto |D_{\pm 1, 0}^2(\theta)|^2 \propto \sin^2 2\theta, \quad (3)$$

with a maximum at  $45^\circ$  to the beam. If the probability of quadrupole absorption relative to dipole absorption is  $q$ , and the energies of the  $1^-$  and  $2^+$  states relative to the lowest barrier are  $E_{1^-}$  and  $E_{2^+}$ , then the probability of fission from quadrupole states relative to dipole states is given by

$$Q = q \frac{P(E_{\text{exc}} - E(2+))}{P(E_{\text{exc}} - E(1-))} = q \frac{P(E_{\text{exc}} - E(2+))}{P(E_{\text{exc}} - E(2+) - \Delta)}, \quad (4)$$

where  $P(E)$  represents the probability of barrier penetration at an energy  $E$  in excess of the barrier, and  $\Delta = E(1^-) - E(2^+)$ .

A calculation of Hill and Wheeler<sup>9</sup> gives

$$P(E) = (1 + e^{-2\pi E/\hbar\omega_c})^{-1} \quad (5)$$

for energies near the maximum of a parabolic barrier. The experiments of Stokes and Northrup<sup>10</sup> indicate that  $\hbar\omega_c$  is approximately 0.6 Mev. Then for  $E_{\text{exc}} = E(2^+)$  and  $q \sim 10^{-2}$ ,  $\Delta$  need only be about  $\frac{1}{2}$  Mev to allow quadrupole fission to compete successfully with dipole fission. However, such competition will exist only over an energy range of the order of  $\Delta$ , since the ratio  $Q$  approaches  $q$  for values of  $E_{\text{exc}} > E_{1^-}$ . At energies in excess of the fission barriers for both the  $2^+$  and  $1^-$  states, the larger probability for dipole absorption of the photon should guarantee the dominance of the dipole distribution (2) in the anisotropy. At still higher

energies (millions of volts in excess of the lowest fission barrier), one expects that various channels, characterized by  $K=1$  and  $K=2$  as well as  $K=0$ , will be available to carry the nucleus to fission, so that the angular distribution should become isotropic as observed.

The fact that near threshold the magnitude of the quadrupole component in the angular distribution can supply information bearing upon the difference  $\Delta$  between the lowest lying state of  $1^-$  character and the  $2^+$  member of the first rotational band has implications for the resonance fission of odd- $A$  targets by slow neutrons. For  $U^{235}$  ( $\frac{7}{2}^-$ ), a compound nucleus is formed which has an excitation energy  $E^*$  about 1.0 Mev greater than the lowest fission barrier and parity either  $3^-$  or  $4^-$  (see Fig. 1). For resonances with the  $3^-$  character, fission should occur predominantly through the  $3^-$  member of the lowest rotational band. On the assumption that  $\Delta$  is small compared to 1 Mev, one might expect<sup>11</sup> that such fissions should exhibit (a) larger than average fission widths, because the excitation energy is well above this  $3^-$  barrier; and (b) less than average probabilities for symmetric fission, because the lowest  $3^-$  state is supposed to be in a state of asymmetric vibration characterized by a node at the symmetric shape.

The so-called "wheel" experiment of Cowan and associates<sup>12</sup> bears out suggestion (b) above, but a careful study of 51 fission and absorption resonances by Havens<sup>13</sup> does not offer any support for suggestion (a).

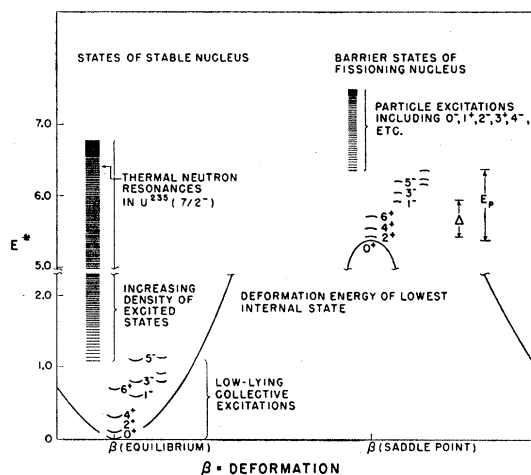


Fig. 1. The structure of the fission barrier of an even-even nucleus. The numerical scales are appropriate to  $U^{236}$ . Also indicated is the excitation energy of the nucleus after absorption of a thermal neutron by  $U^{235}$ .

<sup>7</sup> Winhold, Demos, and Halpern, *Phys. Rev.* **87**, 1139 (1952).  
<sup>8</sup> Katz, Baerg, and Brown, *Proceedings of the Second United Nations International Conference on the Peaceful Uses of Atomic Energy, Geneva, 1958* (United Nations, Geneva, 1959), Paper No. P/200.

<sup>9</sup> D. Hill and J. Wheeler, *Phys. Rev.* **89**, 1102 (1953).

<sup>10</sup> R. Stokes and J. Northrup, *Proceedings of the Second United Nations International Conference on the Peaceful Uses of Atomic Energy, Geneva, 1958* (United Nations, Geneva, 1959), Paper No. P/582.

<sup>11</sup> See John A. Wheeler, *Proceedings of the International Conference on Nuclear Reactions, Amsterdam, 1956* (Nederlandse Natuurkundige Vereniging, Amsterdam, 1956); also Oak Ridge National Laboratory Report ORNL-2309, 1956 (unpublished). Wheeler suggests alternative explanations but none which is subject to as immediate a test as that proposed here.

<sup>12</sup> G. A. Cowan, *Bull. Am. Phys. Soc.* **4**, 31 (1959).

<sup>13</sup> W. Havens (private communication).

These observations could be made consistent if the separation,  $\Delta$ , between the lowest lying rotational states and the lowest odd-parity states were not assumed small (see Fig. 1) but instead were comparable to the energy  $E_P$  required to excite particle states. Then the barrier heights for the  $3^-$  and  $4^-$  states would be comparable, leading to comparable average fission widths. However, the state ( $3^-$ ) corresponding to the excited asymmetric vibration would still exhibit the stronger tendency towards asymmetric fission.

The relevance of these resonance data to the photofission of  $U^{236}$  is obvious. If  $\Delta$  is large, the situation is of the kind favorable to the appearance of a quadrupole component in the photofission fragment angular distribution at energies slightly above the lowest threshold (about 5.5 Mev).

## 2. Photofission of Odd-Even Targets

The anisotropy to be expected from photofission of unoriented odd-even targets depends more specifically on the details of the spectrum at the barrier. Basically, it is the quantization of the  $Z$  component of angular momentum ( $M = \pm 1$ ) of the photon which allows one to form an anisotropic distribution of compound nuclear angular momenta in photon absorption. When the target has a nonzero spin, this spin must be added to the photon angular momentum to obtain the compound nuclear spin. Clearly, if the target spin is greater than 1, the resulting distribution of compound nuclear spins will not be very anisotropic, and the maximum fragment anisotropy will be correspondingly small.

For a target with spin  $\frac{1}{2}$ , however, a measurable fragment anisotropy might result if the low-lying spectrum at the barrier were favorable. In such a case, dipole absorption of the photon would yield compound states  $(I, M) = (\frac{3}{2}, \pm\frac{3}{2}), (\frac{3}{2}, \pm\frac{1}{2}), (\frac{1}{2}, \pm\frac{1}{2})$  in the proportion 3, 1, 2. Then the anisotropy just above threshold would depend on whether a  $K = \frac{3}{2}$  band or a  $K = \frac{1}{2}$  lies lower; one calculates

$$W(0^\circ)/W(90^\circ) = 2.0$$

for fission through the  $K = \frac{3}{2}$  band only, and

$$W(0^\circ)/W(90^\circ) = 0.572$$

for fission through the  $K = \frac{1}{2}$  band only. If both  $K = \frac{3}{2}$  and  $K = \frac{1}{2}$  states lie low (a not unlikely situation), the anisotropy would be considerably less than either of these maximal estimates. Moreover, the observation of this anisotropy would require a rather precise definition of the energy of the photon causing fission, since the spacing between bands of different  $K$  just above threshold is probably  $< \frac{1}{4}$  Mev, in contrast to the even-even case where one expects to find mostly  $K = 0$  states until sufficient excitation ( $\sim 1$  Mev) is available to break a pair.

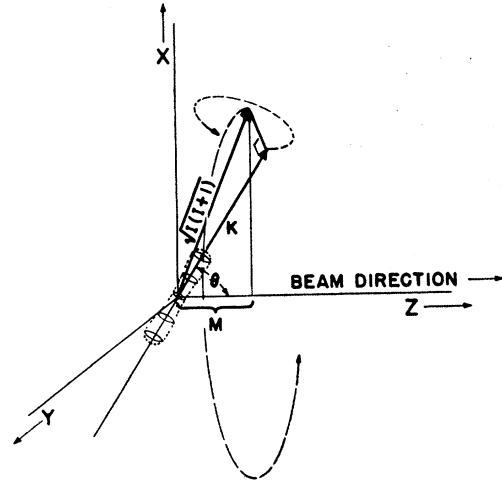


FIG. 2. The classical analog of the orientation of the nuclear symmetry axis (parallel to  $K$ ) when the total angular momentum is  $I$ , the  $Z$  component is  $M$ , and the projection along the nuclear symmetry axis is  $K$ . Classically,  $K$  precesses around  $I$  as shown by the small circle, and  $I$  is distributed about the beam axis with equal probability as shown by the large circle. The resulting distribution of orientations for the symmetry axis is given by Eq. (8).

## 3. Neutron-Induced Fission

In contrast with photons, neutrons of moderate energy are capable of forming compound states with a variety of spins due to the large orbital angular momentum which they can contribute in collisions with the nucleus. Moreover, this orbital angular momentum is perpendicular to the neutron beam so that only the intrinsic spin of the projectile is available to modify the  $Z$  component of angular momentum of the target. Thus, for neutrons with kinetic energies of one or more millions of volts incident on even-even targets, the compound nuclei, considered classically, have their angular momentum restricted to cones whose base is perpendicular to the beam, as shown in Fig. 2. As they pass over the barrier to fission through some channel with a given value of  $K$ , the distribution of the symmetry axis is space is given by

$$W_K(\theta) = \sum_{I, M = \pm \frac{1}{2}} G(I, M) |D_{MK}^I(\theta)|^2, \quad (6)$$

where  $G(I, M)$  is the probability of forming a compound nucleus of angular momentum  $I$  and  $Z$  component  $M$  in the bombardment. When fission can occur through a variety of channels of different  $K$  with a probability  $F(K)$ , the observed angular distribution will be of the form

$$W(\theta) = \sum_K F(K) W_K(\theta) = \sum_{K; I, M = \pm \frac{1}{2}} F(K) G(I, M) |D_{MK}^I(\theta)|^2. \quad (7)$$

For large values of  $I$ , the square of a  $D$  function describes, on the average, the distribution of a classical

vector of length  $K$  which precesses at a constant rate about the fixed vector  $I$ .<sup>14</sup> The end point of the vector  $I$ , in turn, is distributed about the beam axis with uniform probability in the polar angle, as shown in Fig. 2. Thus, if the process involves averages over several values of  $I$  and  $K$ , one may substitute the classical distribution<sup>15</sup>:

$$|D_{MK}^I(\theta)|^2 \propto \left[ \sin^2\theta - \frac{K^2 + M^2}{I(I+1)} + \frac{2KM}{I(I+1)} \cos\theta \right]^{-\frac{1}{2}} \quad (8)$$

If, furthermore,  $M$  is small compared to  $I$  and  $I$  is much larger than 1, as in the case of fission by energetic neutrons, one can set  $M=0$  to obtain the classical approximation of Bohr:

$$|D_{0K}^I|^2 \propto \begin{cases} [\sin^2\theta - (K^2/I^2)]^{-\frac{1}{2}}, & \sin\theta > K/I \\ =0, & \sin\theta \leq K/I. \end{cases} \quad (9)$$

In this approximation, one has

$$W(\theta) = N \int_0^{I_{\max}} \int_{K < I \sin\theta}^{K_{\max}} \frac{F(K)G(I)}{(\sin^2\theta - K^2/I^2)^{\frac{1}{2}}} dK dI, \quad (10)$$

where  $N$  is a normalization factor.<sup>16</sup> The sums have been replaced by integrations, and the functions  $F$  and  $G$  are now to be considered continuous functions of their variables.

It should be noted that the limits of integration in Eq. (10) are defined in a manner equivalent to the restriction that  $F(K)=0$  for  $K > I \sin\theta$ . One is, therefore, free to discuss  $F(K)$  entirely in terms of the spectrum at the barrier without reference to the  $I$  values made available by any specific process of forming the compound nucleus.

To specify the probability  $G(I)$  of forming a compound state with angular momentum  $I$ , where  $I$  is equal to the neutron angular momentum  $L$ , we assume the classical distribution for  $L$ . Then

$$G(I) \propto \begin{cases} I, & I \leq L_{\max} \\ =0, & I > L_{\max}; \end{cases} \quad (11a)$$

$$\hbar(L_{\max} + \frac{1}{2}) = MvR = (2ME_N)^{\frac{1}{2}}R = \hbar k_n R, \quad (11b)$$

where  $Mv$  is the (classical) momentum of a neutron with energy  $E_n$ , and  $R$  is the nuclear radius. The addition of  $\frac{1}{2}$  in (11b) represents a rough correction for the fact that the neutron penetration factor  $T_l$  does not approach unity<sup>17</sup> until  $l$  exceeds  $k_n R$  by approximately that amount.

<sup>14</sup> See E. P. Wigner, *Group Theory and Its Application to Atomic Spectra* (Academic Press, Inc., New York, 1958).

<sup>15</sup> The distributions (8) and (9) apply only for angles where they yield a real probability. The classical theory allows no emission at angles for which (8) or (9) are imaginary.

<sup>16</sup>  $N$  is a function only of  $K_{\max}$  and  $I_{\max}$  and therefore cancels in all calculations of the anisotropy  $W(0^\circ)/W(90^\circ)$ .

<sup>17</sup> See J. M. Blatt and V. F. Weisskopf, *Theoretical Nuclear Physics* (John Wiley and Sons, New York, 1952), p. 362.

The accuracy of these appropriations is assessed in Sec. IV.3 by comparison with detailed calculations based on Eq. (7).

The function  $F(K)$  specifies the probability that the fission occurs through a state at the barrier with projection  $K$  of total angular momentum along the symmetry axis. It is, therefore, proportional to the number of such states at the barrier which are energetically available for fission, weighted with the barrier penetration probability of each state. In the spirit of the classical approximation, we assume that the penetration probability is unity if  $E_{\text{exc}} \geq E_K$  and zero otherwise. Then the form of  $F(K)$  is determined by the distribution of states  $K$  at the barrier with energy below the excess excitation energy  $E_{\text{exc}}$ .

If the excitation energy in excess of the barrier is small, the distribution in  $K$  for an odd-mass compound will resemble that of single-particle states in a strongly deformed nucleus. Curve (a) of Fig. 3 shows the number of such states which arise from a given spherical oscillator shell<sup>18,19</sup> as a function of  $K$ .

For very large deformations, states from different major oscillator shells will be thoroughly intermingled; thus, it is reasonable to assume that the distribution in  $K$  is approximately of the form [curve (b) of Fig. 3]:

$$F(K) \propto \begin{cases} K - K_{\max}, & K \leq K_{\max} \\ =0, & K > K_{\max}. \end{cases} \quad (12)$$

$K_{\max}$  here is expected to increase with increasing energy above the barrier.

If the compound nucleus' excitation energy in excess of the lowest barrier is large, then one can utilize

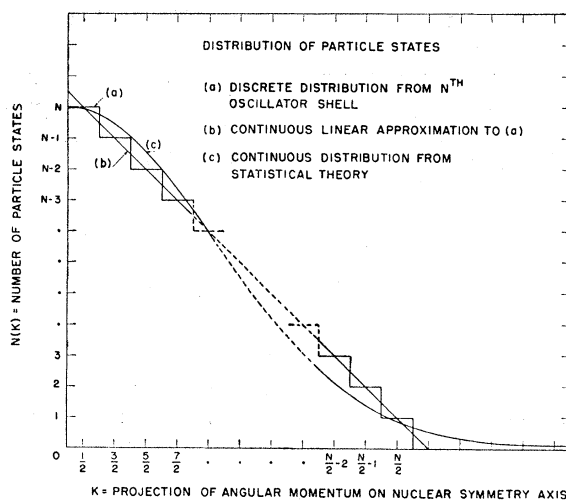


Fig. 3. The number of particle states of a given  $K$  vs  $K$ . Each of the three curves has the same  $\bar{K}$  (average value of  $K$ ). The figure shows that the three distributions are approximately equivalent if  $\bar{K}$  is chosen the same in each (see reference 19).

<sup>18</sup> See S. G. Nilsson, *Kgl. Danske Videnskab. Selskab, Mat.-fys. Medd.* **29**, No. 16 (1955).

<sup>19</sup> Torlief Ericson, *Nuclear Phys.* **6**, 62 (1958).

statistical considerations in discussing the probability distribution of  $K$  at the barrier. The energy  $E_{\text{exc}}$  will appear at the barrier (a) in the form of collective kinetic energy,  $\epsilon$ , of the motion towards fission and (b) in the form of internal excitation,  $E$  (including intrinsic, rotational, and vibrational excitation). Then

$$E_{\text{exc}} = E + \epsilon. \quad (13)$$

Let  $\rho_{\text{int}}(E, K)$  be the density of internal states which at an excitation energy  $E$  have a projection  $K$  of angular momentum along the symmetry axis:

$$\rho_{\text{int}}(E, K) = P(K, E)\rho(E), \quad (14)$$

where  $\int_0^\infty P(K, E) dK = 1$  and  $\rho(E)$  is the total density of internal states at excitation energy  $E$ . The density of collective kinetic energy states is given by

$$\rho_{\text{kin}}(\epsilon) d\epsilon \propto \epsilon^{-\frac{1}{2}} d\epsilon, \quad (15)$$

provided the path towards fission is one-dimensional. Then the total number of states of projection  $K$  leading to fission is

$$N_K(E_{\text{exc}}) \propto \int_0^{E_{\text{exc}}} d\epsilon \int_0^{E_{\text{exc}}} dE [P(K, E)\rho(E)\epsilon^{-\frac{1}{2}}] \times \delta(\epsilon - (E_{\text{exc}} - E)), \quad (16)$$

where the  $\delta$  function introduces the constraint (13). The probability of fission through a state with projection  $K$  is therefore

$$F(K, E_{\text{exc}}) = \int_0^{E_{\text{exc}}} dE [P(K, E)\rho(E)(E_{\text{exc}} - E)^{-\frac{1}{2}}] \div \int_0^{E_{\text{exc}}} dE [\rho(E)(E_{\text{exc}} - E)^{-\frac{1}{2}}]. \quad (17)$$

Since  $\rho(E)$  is a rapidly increasing function of  $E$  and since  $(E_{\text{exc}} - E)^{-\frac{1}{2}}$  is large at  $E \approx E_{\text{exc}}$ , one expects that contributions to the integral in the numerator will come chiefly from the neighborhood of  $E = E_{\text{exc}}$ . Then the slowly varying factor  $P(K, E)$  can be evaluated at  $E = E_{\text{exc}}$  to obtain approximately

$$F(K, E_{\text{exc}}) \simeq P(K, E_{\text{exc}}). \quad (18)$$

For excitation energies far in excess of the barrier, statistical theory<sup>19,20</sup> predicts that  $P(K, E_{\text{exc}})$  is a normal distribution [curve (c), Fig. 3]:

$$F(K) \propto \exp[-(K^2/\pi\bar{K}^2)], \quad (19)$$

where  $\bar{K}$  is the average value of  $K$ . Statistical theory also predicts that  $\bar{K}$  is proportional to  $(E^* - E_f)^{\frac{1}{2}}$ . Neither this distribution nor this energy dependence of  $\bar{K}$  has been utilized in any of the calculations reported here. Figure 3 indicates that the linear distribution which was assumed should give essentially the same

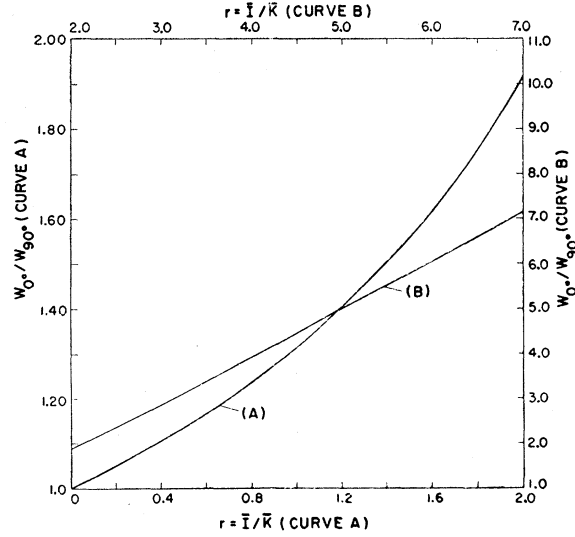


FIG. 4. The function  $W(0^\circ)/W(90^\circ)$  vs the ratio  $r = \bar{I}/\bar{K}$ . The analytical expression for  $W(0^\circ)/W(90^\circ)$  is given in Eqs. (20) and (20a).

results as the normal distribution.<sup>21</sup> The assumed energy dependence of  $\bar{K}$ , which is most crucial in determining the dependence of the anisotropy on energy, is discussed below.

The expression (10) for the ratio  $W(0^\circ)/W(90^\circ)$  which results from the assumed linear distribution in  $K$  is integrable analytically, and depends only on the ratio  $r = \bar{I}/\bar{K}$ . The result is

$$W(0^\circ)/W(90^\circ) = (1 - 3r/4\pi)^{-1}, \quad r \leq 2 \quad (20) \\ = (\pi/6) \left\{ \frac{1}{3} \sin^{-1}(2/r) - \frac{1}{8} [r - (r^2 - 4)^{\frac{1}{2}}] \right. \\ \left. + (1/12r^2)(r^2 - 4)^{\frac{1}{2}} \right. \\ \left. + (1/3r^3) \ln \frac{1}{2} [r + (r^2 - 4)^{\frac{1}{2}}] \right\}^{-1}, \quad r \geq 2. \quad (20a)$$

This expression is displayed graphically in Fig. 4. For an assumed energy dependence of  $\bar{K}$ , Eqs. (11) and Fig. 4 allow one to predict the energy dependence of  $W(0^\circ)/W(90^\circ)$ .

If the excitation energy exceeds the neutron binding energy, competition from neutron evaporation must be included. Of the compound nuclei of mass  $A+1$  formed initially, a fraction  $\gamma_{A+1} \equiv \Gamma_f/(\Gamma_n + \Gamma_f)$  undergo fission ("first-chance" fission), and the remaining fraction  $1 - \gamma_{A+1}$  emits neutrons to form nuclei of mass  $A$ . If there is still sufficient excitation energy

<sup>21</sup> The angular distributions based on Eqs. (12) and (19) differ somewhat. The former is  $W(\vartheta) \propto 4\pi r^3 - 3r^2 \sin^2 \vartheta$  for  $r \leq 2$ . It differs from the latter [given by V. M. Strutinskii, *Atomnaya Energ.*, **2**, 508 (1957) [translation Soviet J. Atomic Energy **2**, 621 (1957)]] in that it has a finite slope at  $\vartheta = 0$  and yields lower emission probabilities for intermediate angles, from say,  $30^\circ$  to  $60^\circ$ . The first difference disappears when the neutron and/or target spin is taken into account (see Fig. 11). As regards the second difference the data of Blumberg *et al.* (reference 25) on  $\text{Pu}^{239}$  might be interpreted as favoring the former distribution for values of  $E_{\text{exc}}$  up to 3 Mev.

<sup>20</sup> C. Bloch, *Phys. Rev.* **93**, 1094 (1954).

remaining for fission to occur,  $\gamma_A[1-\gamma_{A+1}]$  nuclei of mass  $A$  will undergo fission ("second-chance" fission). This process continues until the excitation energy is less than the fission and neutron emission thresholds. Subsequent decay is by gamma cascade, neglected here when competition from fission and neutron emission is energetically possible. The anisotropy is then a sum of the anisotropies for the different fissioning species, weighted by the number of fissions associated with each species.

#### 4. Low Energy

We first discuss the qualitative features of fission anisotropy for neutrons of energy less than 12 Mev. In this region, differences between even-even and odd-mass targets may be attributed primarily to differences in the fission thresholds. (The fission of odd-odd nuclides is omitted to simplify the presentation. The appropriate extensions to such cases should, however, be obvious.)

Even-even targets have positive thresholds for fission of the order of 1 Mev. Since neutrons of this energy form compound states with  $\bar{I} \approx 1.0$ , one expects in general that not too far above threshold where  $\bar{K}$  is still small, significant forward peaking will be observed. Also, as the energy increases above threshold,  $\bar{K}$  will increase more rapidly than  $\bar{I}$ , leading to an anisotropy decreasing with energy.

At that energy where fission after neutron emission becomes possible, the second-chance fissions occur with energy barely in excess of the barrier and with a relatively small value of  $\bar{K}$ . The distribution of  $I$ , on the other hand, is changed only to the extent that the emitted neutrons carry off angular momentum. Since the neutrons are emitted chiefly in  $S$ -wave states, this is a small effect which can be neglected in a first approximation. The second-chance fissions are, therefore, characterized by a large ratio,  $\bar{I}/\bar{K}$ , and increased forward peaking is observed to set in with second-chance fissions. With further increase in neutron energy, the excitation increases, increasing the average component of angular momentum along the symmetry axis, and resulting in a diminution of the tendency towards forward peaking.

Exceptions to this picture may be expected where strong deviations from the assumed distribution of  $K$  occur. Such situations can arise in the neighborhood of the fission threshold. Thus, when the fissioning species is an odd-mass nuclide, the appropriate value of  $\bar{K}$  for fissions occurring predominantly through the first rotational band is just the value of  $K=K_1$  associated with that band. Moreover, fissions can occur only from compound nuclei whose total angular momentum is consistent with those of the rotational states energetically available:  $K_1, K_1+1, \dots, I$ . Then fission may occur only through a few states with  $K$  approximately equal to  $I$ . The fragments will be emitted in the

direction  $90^\circ$  to the beam, as has been observed<sup>22</sup> in  $\text{Th}^{232}$ . Wilets and Chase<sup>23</sup> have made a detailed analysis of this case in terms of the Bohr model. The statistical treatment discussed in this paper cannot include such special cases. It applies only to circumstances where one expects averages over many barrier states to determine the situation. Such should be the case for excitations greater than  $\sim 1$  Mev above the fission threshold.

Odd-even targets are often thermally fissionable. This implies that even for zero-energy neutrons, the quantity  $E^*-E_f$  is positive. As a result, the first-chance peak in the anisotropy is inaccessible via neutron bombardment, so that one observes at a given energy a much lower anisotropy than the corresponding even-even value.

Odd-even targets differ from even-even targets also in that they have a finite spin which must be combined with the neutron angular momentum to obtain the spin of the compound nucleus. The effect of target spin on anisotropy is discussed separately in Sec. IV.3. For most of the estimates reported here, the target spin has been assumed to be zero.

#### 5. Higher Energy

For higher bombarding energies, the anisotropy is a composite of anisotropies due to the various species of the chain formed by successive neutron emissions. We discuss next the qualitative features of the dependence on anisotropy with energy in this region.

Since evaporated neutrons carry off only a small angular momentum, the distribution of compound nuclear angular momenta involved in the fission of various species in the chain is approximately the same as that in the initial compound system. In contrast, the excitation energy of the fissioning nuclide decreases significantly with each neutron emission. Therefore, just above its threshold, last-chance fission is characterized by  $\bar{I}$  at formation but by a low excitation energy at the barrier (i.e., a low  $\bar{K}$ ), a combination which implies a large anisotropy. Thus, one expects a sudden increase in the overall anisotropy as each new  $(x, xn'f)$  process becomes energetically possible; namely, at energy intervals of  $\sim 6$  Mev.

The over-all 6-Mev cycle will be influenced by other effects which can be described within the present classical-statistical description. Two such effects are fissionability and odd-even alternation. These affect the anisotropy chiefly by their influence on the number of  $(x, xn'f)$  processes which occur. We discuss them separately.

In a nucleus whose fission half-life is long compared with neutron emission times, there will be approximately the same number of first-, second-, etc., chance fissions. Then considering this effect alone, one expects

<sup>22</sup> J. Brolley and R. Henkel, Phys. Rev. **103**, 1292 (1956).

<sup>23</sup> L. Wilets and D. Chase, Phys. Rev. **103**, 1296 (1956).

a pattern like the solid curve of Fig. 5, where the number of fissions and the anisotropy associated with  $n$ th-chance fission is assumed independent of  $n$ . In the opposite extreme of short fission lifetime, all fissions are first-chance fissions, and only the first peak would be seen. Real nuclides are, of course, intermediate to these extremes. Moreover, as neutrons are emitted,  $Z^2/A$  increases, tending in general to increase the proportion of  $n$ th-chance fission along the chain; also, as fissions occur, the compound nucleus is depleted, tending to decrease the proportion of  $n$ th-chance fission. Finally, the spread of excitation energy in fissioning nuclides left after several neutron emissions tends to smear the sharp structure more and more as the number of emitted neutrons increases.

Odd-even alternation manifests itself (a) in a lower average value of  $\bar{K}$  when the fissioning nucleus is even-even and (b) in alternation of the sign of the difference,  $E_F - E_N$ , between the fission threshold and the neutron binding energy from even-even to odd-mass nuclei. Effect (a) would imply that at the same moderate excitation, an even-even nucleus should show a stronger tendency towards forward peaking than an odd-even nucleus. This is especially true if the excitation is less than the pairing energy so that the available fission channels in the even-even tend to have  $K=0$ . Effect (b) allows even-even nuclides left with excitation energy in the range  $E_F < E_{exc} < E_N$  to fission with competition only from  $\gamma$  emission. Under circumstances where a significant fraction of the neutron decays from the preceding member of the chain leave a nuclide with excitation energy in this range, the proportion of fissions following this emission to total fissions will be anomalously high.<sup>24</sup> Both effects (a) and (b) tend to

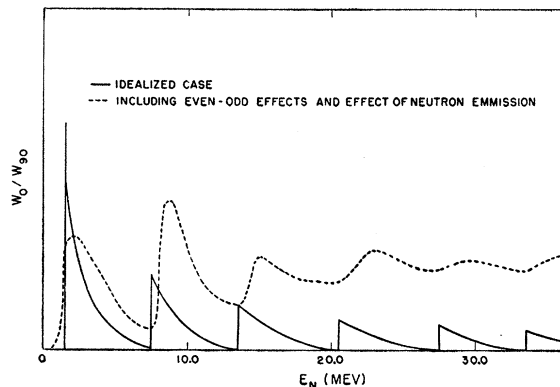


FIG. 5. Qualitative dependence of anisotropy on neutron energy. The solid curve is a highly schematized representation in which the anisotropy reaches its peak immediately above threshold and becomes zero just before the next-chance fission sets in. The dashed curve is a qualitative illustration which attempts to illustrate various detailed effects discussed in the text.

<sup>24</sup> This effect has been discussed by Jackson in connection with the tendency of the fission cross section to "overshoot" the plateau associated with the fission of an even-even compound. See J. D. Jackson, Proceedings of the Symposium on the Physics of Fission, Chalk River, Canada, 1956 (unpublished).

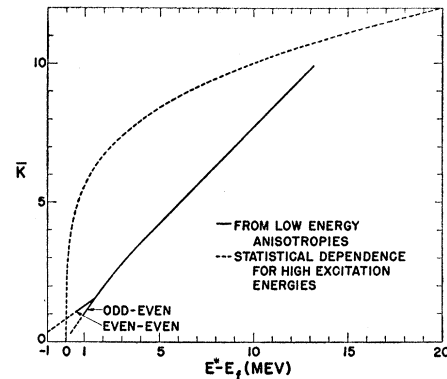


FIG. 6. The dependence of  $\bar{K}$  on  $E^* - E_f$  as obtained from the anisotropy of  $\text{Pu}^{239}(n, f)$  and  $\text{U}^{238}(n, n'f)$ . Also shown (dashed curve) is the dependence implied by the continuum statistical theory, which should be valid at high excitation energies. To apply this figure to even-even nuclei, 1 Mev should be subtracted from  $E^*$ .

enhance the anisotropy for even-even nuclides relative to odd-even nuclides.

In the solid curve of Fig. 5, it has been assumed that the distribution becomes isotropic for excitations more than 6 Mev in excess of the barrier. This, in fact, is not the case. The dotted curve, though still qualitative, is a more realistic representation which includes a contribution to the anisotropy from earlier members of the chain and attempts as well to indicate the smearing of the sharp structure due to the spread in energy of the emitted neutrons.

### III. NUMERICAL ESTIMATES

Numerical estimates of the neutron-induced fission fragment anisotropy have been made on the basis of the model discussed above. Of the elements needed to estimate the anisotropy, the most crucial is the dependence of  $\bar{K}$  on energy. Indeed, the utility of the theory depends largely upon whether or not a single curve of  $\bar{K}$  vs energy can be found which gives a satisfactory description of the anisotropy for a variety of fissioning nuclides.

We have determined a function  $\bar{K}(E^* - E_f)$  for excitations between 1.6 and 5 Mev from the measurements of Blumberg *et al.*<sup>25</sup> on  $\text{Pu}^{239}$ . These data have considerably smaller statistical error than any previously published work. Since the spin of  $\text{Pu}^{239}$  is only  $\frac{1}{2}$ , one expects its effect to be small, even for neutron energies of only 1 Mev. Above 5 Mev,  $\bar{K}(E^* - E_f)$  was extended linearly as shown in Fig. 6, and the implied anisotropies were compared with the experimental data as a test of the extrapolation. As will be discussed below, probable errors in estimated thresholds and ambiguity in the manner of treating even-even compounds vis-à-vis odd-even compounds at very low excitation energies introduce enough uncertainty into

<sup>25</sup> L. Blumberg *et al.*, Bull. Am. Phys. Soc. 4, 31 (1958). A more complete report is to be published.

TABLE I. Assumed thresholds.

Nuclide	$E_{(n,f)}$ (Mev)	$E_{(n,n'f)}$ (Mev)
Pu <sup>239</sup>	-1.6	5.7
U <sup>233</sup>	-1.6	5.3
U <sup>238</sup>	1.2	5.5
Th <sup>232</sup>	1.4	5.9

the numerical estimates to render fruitless any further refinement of the assumed curve on the basis of present data.

Also shown in Fig. 6 is the form of  $\bar{K}(E^*-E_f)$  implied by continuum statistical theory. This curve should become applicable at high excitation energies, and presumably does so at excitation energies several Mev greater than the highest considered here (13 Mev). A curve qualitatively similar to the combination of our low-energy curve and the statistical curve at higher energies has been used in similar calculations by Halpern and Strutinskii.<sup>26</sup>

Besides the dependence of  $\bar{K}$  on  $E^*-E_f$ , other assumptions are required to reduce the theory to numerical estimates. These concern the values of fission barrier energies, the differences between even-even and odd-even compounds at a given excitation, the spectrum of evaporated neutrons, and the proportion of second chance fissions. Since these can, in some cases, affect the calculated anisotropy significantly, we have chosen certain definite prescriptions for specifying each of them. Later, the effects of tenable alternatives will be discussed.

The prescriptions adopted are listed below. Thresholds used are estimates of the energy at which the penetration probability through the lowest barrier state is equal to one-half [see Eq. (5)]; they are summarized in Table I.

(1) For even-even compound nuclei, one Mev is subtracted from the excitation energy in estimating

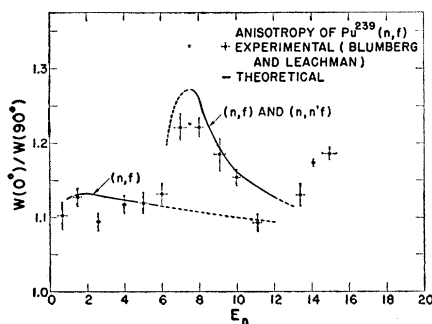


FIG. 7. Theoretical and experimental anisotropies for Pu<sup>239</sup>. The theoretical curves (solid lines) assume  $I_0=0$ . The asterisks at the energy corresponding to the peak of the second-chance anisotropy indicate the effect of changing the assumed  $(n,n'f)$  threshold by  $\pm 0.4$  Mev.

<sup>26</sup> I. Halpern and V. Strutinskii, *Proceedings of the Second United Nations Conference on the Peaceful Uses of Atomic Energy, Geneva 1958* (United Nations, Geneva, 1959), Paper No. P/1513.

$\bar{K}$ .<sup>19</sup> For very low excitations, a different dependence of  $\bar{K}$  on  $E^*-E_f$  is assumed for even-even nuclei from that for odd- $A$  nuclei (see Fig. 6).

(2) Thresholds and proportions of second-chance fissions are estimated from measured cross section data.<sup>10,27</sup> In estimating the proportion of second-chance fission, the value of the cross section on the first plateau is assumed to determine the first-chance contribution.

(3) Fission is assumed to compete with energetically allowed neutron emission only if the excitation energy exceeds the fission barrier by 0.3 Mev.

(4) In estimating the excitation energy for second-chance fissions, evaporated neutrons are assumed (a) to carry no angular momentum and (b) to be monoenergetic with kinetic energy equal to the average kinetic energy of the neutrons which leave enough energy for subsequent fission to occur. A Maxwell distribution<sup>28</sup> with  $\tau=0.75$  Mev is used to evaluate this average.

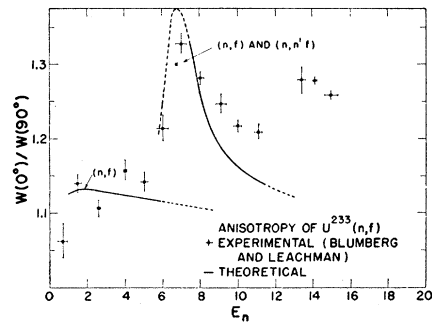


FIG. 8. Theoretical and experimental anisotropies for U<sup>233</sup>. The anisotropy calculated on the assumption that the  $(n,n'f)$  threshold was 0.4 Mev greater than that in Table I would be 1.41, which falls beyond the range of the figure.

#### IV. DISCUSSION OF NUMERICAL ESTIMATES

The numerical estimates of anisotropy  $vs$  energy are given in Figs. 7, 8, 9, and 10, together with the relevant data.<sup>25,29-33</sup> We shall discuss the first- and second-chance estimates separately.

##### 1. First-Chance Fission Anisotropies

The low-energy dependence of  $\bar{K}$  for odd-even compound nuclei was determined by fitting the data on Pu<sup>239</sup> in the manner shown in Fig. 7. Neglecting the spin and assuming the same fission threshold for U<sup>233</sup>, one calculates the same anisotropy for those two nuclides.

<sup>27</sup> R. L. Henkel, *Fast Neutron Physics* (Interscience Publishers, Inc., New York, to be published).

<sup>28</sup> See reference 17, p. 368.

<sup>29</sup> R. Henkel, Los Alamos Scientific Laboratory Report LA-2122 (unpublished).

<sup>30</sup> W. Dickinson and J. Brolley, *Phys. Rev.* **90**, 388 (1953); **94**, 640 (1954).

<sup>31</sup> Brolley, Dickinson, and Henkel, *Phys. Rev.* **99**, 159 (1955).

<sup>32</sup> R. Henkel and J. Brolley, *Phys. Rev.* **103**, 1292 (1956).

<sup>33</sup> Simmons, Henkel, and Brolley, *Bull. Am. Phys. Soc. Ser. II*, **2**, 308 (1957).

This agrees with the experimental results to within a few percent as shown in Fig. 8, in contrast to the expected effect of the spin, as will be discussed in Sec. IV. 3.

The first-chance anisotropy calculated for the targets  $\text{Th}^{232}$  and  $\text{U}^{238}$  from the same assumed  $\bar{K}$  dependence is shown in Figs. 9 and 10. One sees that the agreement is moderately good. Also, it could be improved by slight changes in the assumed values of the fission threshold  $E_f$  which effect primarily a shift in energy of the calculated anisotropy.

The dotted portions of the curves indicate regions either where the estimated value of  $\bar{K}$  was less than one (so that reservations must be retained concerning the hypothesized distribution) or where the energy concerned is above the second-chance threshold.

## 2. Second-Chance Fission Anisotropies

The estimated second-chance anisotropies for the odd-even targets are seen to be in semiquantitative

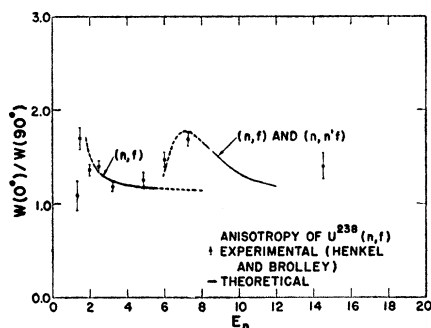


FIG. 9. Theoretical and experimental anisotropies for  $\text{U}^{238}$ .

agreement with the data of Blumberg and Leachman. In this case, the estimated  $\bar{K}$  is greater than one only for bombarding energies greater than approximately 7.5 Mev. We have nonetheless included for its illustrative value the dotted portion of the curve based on the extrapolation of the  $\bar{K}$  dependence to lower values. Actually, the results indicate that such an extrapolation may provide a useful parametrization for the low-excitation anisotropies, even though the statistical assumptions on which they are based retain but little claim to validity.

Since the proportion of second-chance fission is fixed by the measured values of the cross section, as discussed previously, modest changes in the assumed value of  $E_f$  for the second-chance events can effect significant modification of the calculated anisotropy. In Figs. 7 and 8, asterisks have been inserted to indicate the calculated anisotropy at 7.5 Mev if  $E_f$  were changed by  $\pm 0.4$  Mev.

In the case of even-even targets, second-chance fission involves even-even compound nuclei. The subtraction of 1 Mev and of the average energy carried

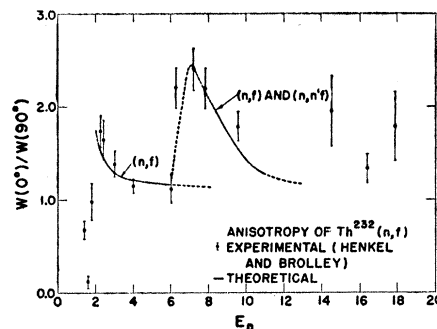


FIG. 10. Theoretical and experimental anisotropies for  $\text{Th}^{232}$ .

by the emitted neutrons leaves an excitation greater than 1 Mev only when the bombarding energy is greater than approximately 8.0 Mev. Thus, the statistical model used here is inadequate to describe the interesting range between 5.5 and 8.0 Mev unless further assumptions are made concerning values of  $\bar{K}$  in even-even nuclides for excitations in the neighborhood of 1 Mev.

The success of the extrapolation to low excitations in the odd-mass targets encourages one to test such assumptions in spite of the fact that the assumed distribution of  $\bar{K}$  cannot adequately describe the situation where only a few barrier states are involved. In assigning a value to  $\bar{K}$  for even-even nuclei of low excitation, one is therefore utilizing the statistical theory merely as a vehicle for parametrizing the anisotropies. Still the procedure is a useful one, since one expects the structure of low-lying excited states in deformed even-even nuclei to be qualitatively the same for various nuclei. For this reason, a parametrization which fits data obtained from one nucleus should also describe others in at least a semiquantitative manner. The measure of the utility of the method will be the variety of fissioning nuclei for which it can be applied successfully.

The low-energy extension of the curve of Fig. 6 marked "even-even" has been chosen to give a fair reproduction of the available data<sup>34</sup> for  $\text{U}^{238}$ . It has then been used to estimate the second-chance anisotropy for  $\text{Th}^{232}$ . As Fig. 10 illustrates, the agreement is quite satisfactory.

The difference between the anisotropies calculated for  $\text{Th}^{232}$  and  $\text{U}^{238}$  is due primarily to the difference in the onset of the second-chance process, as interpreted from measured fission cross sections. The very large anisotropy observed in  $\text{Th}^{232}$  is due chiefly to the gap,  $E_N - E_f \approx 0.4$  Mev, between the neutron binding energy and the fission threshold for  $\text{Th}^{232}$ . Fission of compound nuclei with excitation energy within this gap occurs with especially low excitation energy and without competition from neutron emission.

<sup>34</sup> More complete measurements to be published by R. Henkel and J. Simmons also agree fairly well with the curve of Fig. 9 (private communication from R. Henkel).

To estimate the effect of these low-energy fissions on the anisotropy, we have assumed that the excess in cross section over the value of the cross section at energies ( $>10$  Mev) where the second plateau is approximately constant is to be attributed to fissions in the gap. It is certainly true that this is incorrect just above the threshold where a large fraction of the second-chance fission is fission of nuclei whose excitation lies within this gap, although the cross section still lies below the plateau value. Thus, in particular, the anisotropy estimated at 6.5 Mev is lower than the measured value. This inaccuracy seems a reasonable price to pay for the ability to tie the calculation uniquely to the measured cross section. Alternatives involving one or more parameters which cannot be specified from currently available data seem far less attractive.

### 3. Effect of Target Spin on Fission Anisotropy

To determine the effect of spin, detailed machine calculations have been performed on the basis of Eq. (7) for targets with nonzero spin. We consider a target of spin  $I_0$  and  $Z$  component  $M_0$ . This spin combines with the neutron spin to give channel spin states  $(j, m_j)$ . The channel spin, in turn, combines with the neutron orbital angular momentum ( $L, m_L=0$ ) to form the compound nuclear spin ( $I, M=m_j$ ). We denote the probability that a compound state of spin  $I$  fissions through a channel with projection  $K$  along the nuclear symmetry axis by  $F_I(K)$ , and the probability that the neutron is absorbed with orbital angular momentum  $L$  by  $\bar{w}(L)$ . Then

$$G(I, M, K) = \frac{F_I(K)}{2(2I_0+1)} \sum_{i, L} \bar{w}(L) |C_{m_j 0 M}^{i L I}|^2,$$

where  $C_{\alpha\beta\gamma}^{ABC}$  is a Clebsch-Gordon coefficient. The probability  $\bar{w}(L)$  is of the form

$$\bar{w}(L) = (2L+1)T_L(E_n) / \sum_{L=0}^{L_{\max}} (2L+1)T_L(E_n),$$

where  $T_L$  is the penetration coefficient for  $L$ -wave neutrons of energy  $E_n$ , chosen to resemble the assumed classical distribution (11). To specify the probability of fission through a channel  $K$ , we use the linear distribution (12); then

$$F_I(K) = (K_m - |K|) / \sum_{|K| \leq I} [K_m - |K|], \quad \text{if } K \leq K_m, \text{ and } K \leq I$$

$$= 0, \quad \text{if } K > K_m, \text{ or } K > I.$$

The resulting expression for the angular distribution has been evaluated numerically. The results for several target spins and for a neutron energy of 1.5 Mev are shown in Fig. 11. They show that the anisotropy should

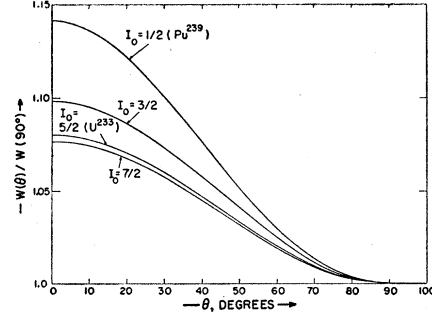


FIG. 11. Theoretical angular distributions of fission fragments, including the effect of target spin. This situation corresponds approximately to those of  $\text{Pu}^{239}$  and  $\text{U}^{233}$  at 1.5 Mev of neutron energy, but does not include corrections arising from consideration of the nuclear deformation discussed in the text.

decrease with increasing spin,<sup>35</sup> provided the excitation energy and the distribution of incoming orbital angular momentum are not changed. In particular, for the comparison of  $\text{U}^{233}$  (spin  $\frac{5}{2}$ ) and  $\text{Pu}^{239}$  (spin  $\frac{1}{2}$ ), the difference in anisotropy should be approximately 6% at 1.5 Mev and 5% at 5 Mev.

This is in contradiction to the data shown in Figs. 7 and 8, where the anisotropy of  $\text{U}^{233}$  is actually larger than that of  $\text{Pu}^{239}$ . Moreover, it would be inconsistent with the measurements of Stokes and Northrup<sup>10</sup> to suppose that the fission thresholds of these targets differ sufficiently to explain such a large deviation from the calculations. Finally, any appeal to a fluctuation away from the expected average values of  $K$  seems to be ruled out by the consistency of the data over the range from 1.5 to 5 Mev.

One possible explanation for the high anisotropy of  $\text{U}^{233}$  relative to  $\text{Pu}^{239}$  is that the process of neutron absorption results in markedly different distributions of compound-nuclear angular momentum for these two nuclides. An effect of this kind could arise from the correlation of the spin direction and the nuclear deformation axis. In classical terminology, one can say that an ellipsoidal target nucleus with a large spin  $I_0$  in a substate  $M_0 \approx 0$  presents its elliptical cross section to the beam while a target with  $M = I_0$  presents a smaller circular cross section. There follows a preference for absorption of neutrons into states with  $M \approx 0$  when the target spin is large, as well as a larger average radius for targets in this substate. This effect would increase the anisotropies over those shown in Fig. 11.

One can make a crude estimate to show that this explanation may indeed be capable of canceling the effect of spin indicated by the more naive calculations leading to Fig. 11. Consider the nucleus to be a classical spheroid with semimajor axis equal to  $\bar{R}(1+\delta)$  and semiminor axes equal to  $\bar{R}(1-\delta/2)$  and oriented at an angle with respect to the neutron beam given by

$$\phi = \cos^{-1} M_0 / [I_0(I_0+1)]^{1/2}. \quad (21)$$

<sup>35</sup> As suggested by Bohr (reference 1).

Then the geometrical cross section in the plane perpendicular to the beam is a function of  $M_0$  given by

$$\sigma(M_0) = \pi \bar{R}^2 (1 + \frac{1}{2}\delta - \frac{3}{2}\delta \cos^2\phi)^{\frac{1}{2}},$$

correct to  $O(\delta^2)$ . If we take the maximum orbital angular momentum absorbed to be proportional to the greatest extension of the nucleus in the plane perpendicular to the beam, this too is a function of  $M_0$  [again correct only to  $O(\delta^2)$ ]:

$$L_m(M_0) = \bar{L}_m [1 + \delta - \frac{3}{2}\delta \cos^2\phi], \quad (22)$$

where  $\bar{L}_m$  is the value which would be obtained from Eq. (11b) for a sphere of radius  $\bar{R}$ .

Assuming  $\delta = 0.25$  and applying the weighting (21) to the angular distributions arising from various values of  $M$  in the calculations summarized in Fig. 11 and estimating the enhancement in anisotropy which Eq. (22) and Fig. 4 imply for the  $M=0$  part, one finds that the correction to the simpler calculation which results from this effect is  $+3\%$  for a target spin of  $\frac{5}{2}$  relative to a spin of  $\frac{1}{2}$ . This is about one-half the magnitude of the expected, but unobserved, suppression of anisotropy for this target spin. The conclusion is that the net effect of target spin will be small, so that in a first approximation one can overlook it entirely. This has been done in the calculations leading to Figs. 7, 8, 9, and 10.

It should be realized that the inclusion of the precession of the nuclear axis about the angular momentum would reduce the difference between the extremes of  $\sigma(M_0)$  and  $L_m(M_0)$  somewhat, leading to a correction smaller than the  $+3\%$  estimated above. On the other hand, a proper wave mechanical treatment of neutron absorption by a deformed nucleus might yield results more consistent with the correction required by the measurements ( $+7\%$ ) than either the crude treatment given here or various refined versions of it can predict.

These detailed calculations are also a useful indicator of the errors involved in the estimates based on Eqs. (10) and (11). The classical approximation to the  $D$  functions appears accurate within  $2\%$  in the anisotropy at this energy, while the use of the distribution (11) in place of more realistic penetration coefficients may introduce as much as  $15\%$  error.<sup>36</sup> However, by determining the average value of  $K$  from observed anisotropies, one certainly compensates for most of this latter error.

#### 4. Correlation Between Mass Asymmetry and Antisotropy

It has been observed in fission by 22-Mev protons<sup>37,38</sup> and in photofission<sup>39</sup> that fragments from the maxima

<sup>36</sup> This statement is based on calculations utilizing the penetration coefficients for uranium given by R. Beyster *et al.*, Los Alamos Scientific Laboratory Report LA-2099, 1957 (unpublished), but retaining the curve  $\bar{K}(E^* - E_f)$  of Fig. 6. It is therefore more an indication of the nonuniqueness of the assumed  $\bar{K}$  values than of the accuracy of calculations based on a given set.

<sup>37</sup> Cohen, Jones, McCormick, and Ferrell, Phys. Rev. **94**, 625 (1954).

<sup>38</sup> Cohen, Ferrell-Bryan, Coombe, and Hullings, Phys. Rev. **98**, 685 (1955).

<sup>39</sup> Fairhall, Halpern, and Winhold, Phys. Rev. **94**, 733 (1954).

of the mass yield curve tend to be more anisotropic than fragments from the valley. In the present model, this qualitative behavior would be expected, not as a correlation between mass division and anisotropy for nuclei fissioning at a single fixed excitation energy, but rather as a correlation between fission events at different excitation energies which occur along the chain. In the observation of fission from a chain of nuclides, selection of a fragment mass which lies in the valley of the yield curve is tantamount to selection of a fission event with a larger than average excitation energy in excess of the barrier, since this mass division is known to become more probable with increasing excitation energy. According to the present model, such an event will show less fragment anisotropy than fissions of lower excitation. Conversely, to choose fragments from the maximum of the mass yield curve is to choose on the average an event of lower average excitation and, therefore, of higher anisotropy.

Data on the correlation between asymmetry and anisotropy in the fission at a well-defined excitation energy, but below the  $(n, n'f)$  threshold, would answer the question of whether or not there is a correlation between anisotropy and mass asymmetry in a fission event at a single fixed excitation energy. Such experimental data would offer evidence on the long-standing question<sup>40-42</sup> of whether symmetric fission arises from traversal of a saddle point in deformation space which is separate and independent of that leading to asymmetric fission, or whether both symmetric and asymmetric fission result from traversal of a single saddle point. In the former case, one would expect different values of the excitation energy at the barrier,  $E_{\text{exc}}$ , for symmetric and asymmetric fission and therefore different angular distributions. Observation of the same angular distributions for various mass divisions would support the original viewpoint of Bohr and Wheeler.

#### 5. General

The success of the Bohr model in fitting anisotropies in a variety of nuclides over a wide range of energies need not be interpreted as evidence that the detailed picture on which Bohr based his assumptions must be accepted. In particular, the work of Strutinskii<sup>2</sup> shows that elimination of the assumption that the barrier spectrum is quasi-stationary does not preclude the derivation of an anisotropy of the form (7). It is not clear that a second element of the Bohr picture, the assumption that  $K$  is a good quantum number at the barrier, is valid at high excitation energies.

A cautious point of view on the use of  $K$  as a good quantum number even when its validity is dubious would be that it does provide a convenient parametrization of the behavior of the anisotropy, and one which is expected to correspond to the physical situation

<sup>40</sup> A. Bohr and J. Wheeler, Phys. Rev. **56**, 426 (1939).

<sup>41</sup> R. D. Present and J. K. Knipp, Phys. Rev. **57**, 1188 (1940).

<sup>42</sup> W. Swiatecki, *Proceedings of the Second United Nations International Conference on the Peaceful Uses of Atomic Energy, Geneva, 1958* (United Nations, Geneva, 1959), Paper No. P/651.

at lower excitations. However, further investigation might establish that in observing statistical averages over many states, the probability distribution of  $K$  is a relevant concept, even though the constancy of  $K$  state-by-state may be in doubt, and that this distribution will behave in accordance with the predictions of statistical theory.

#### ACKNOWLEDGMENTS

The author wishes to express his gratitude to his colleagues, Dr. John Manley, Dr. Robert Leachman, Dr. Richard Henkel, and Dr. Lawrence Wilets for their stimulating interest in this work, and to Mrs. J. Powers, Miss D. Cooper, and Mrs. S. Blumberg for their assistance with the numerical computations.

### Tb<sup>150</sup>: A New Terbium Isotope

K. S. TOTH, S. BJØRNHOLM, M. JØRGENSEN, O. B. NIELSEN, AND O. SKILBREID  
*Institute for Theoretical Physics, University of Copenhagen, Copenhagen, Denmark*

(Received May 15, 1959)

A new isotope with a 3.1-hr half-life has been produced in a 60-Mev proton bombardment of natural gadolinium. The isotope has been identified to be Tb<sup>150</sup> by means of a mass separation performed on the chemically purified terbium fraction. Gamma-ray spectra have revealed an intense 640-kev peak belonging to Tb<sup>150</sup> decay. The  $\gamma$  ray is probably the transition from the first-excited to the ground state in Gd<sup>150</sup>.

A NEUTRON-DEFICIENT terbium isotope with a 3.1-hr half-life has been identified to be Tb<sup>150</sup>. The similarity of this nuclide's half-life to that of its neighbor, Tb<sup>149</sup>, (4.1 hr), partially explains why Tb<sup>150</sup> has not been reported previously. The decay of the isotope is followed by at least one characteristic  $\gamma$  ray whose energy is 640 kev. A strong annihilation peak is also associated with its decay, indicating that the new activity emits positrons.

Approximately 150 mg of natural gadolinium oxide were bombarded for 4 hours with 60-Mev protons accelerated in the Uppsala synchrocyclotron. Most of the known neutron-deficient terbium nuclides were produced and, in order to study each of them, individually, a mass separation was performed. The isotope separator used has been described earlier.<sup>1</sup> A small portion (1-2 mg) of the target was placed in the separator immediately after the material had been delivered (12 hours after the termination of the bombardment). The larger portion was first chemically purified, using an ion-exchange technique.<sup>2</sup> The terbium fraction was then placed in the mass separator. The two mass 150 samples, "A" (chemically impure) and "B" (chemically purified), were similar as far as could be determined from their  $\gamma$ -ray spectra and their decay curves. The effectiveness of the chemical separation in the case of the "B" samples was demonstrated by the mass number 159 samples. "A" of mass 159 clearly contained a large amount of the 18-hr Gd<sup>159</sup>, while "B" of the same mass number showed that the relative amount of Gd<sup>159</sup> had decreased by a factor of 50.

Figure 1 shows the  $\gamma$ -ray spectra of the "A" samples of Tb<sup>149</sup>, Tb<sup>150</sup>, and Tb<sup>151</sup>, all taken at the same energy setting of the scintillation spectrometer. The detector of the spectrometer is a 3-in. NaI(Tl) crystal and the spectra are displayed on a 100-channel pulse-height analyzer. A series of  $\gamma$  spectra taken at a constant energy setting facilitates the assignment of  $\gamma$  rays to the various isotopes. It is seen from Fig. 1 that the mass numbers are not quantitatively separated. Indeed, Tb<sup>151</sup> is present in both the 149 and 150 masses. All masses were found to be present to some extent in their neighbors (2-5%). The abundance of Tb<sup>151</sup> in the Tb<sup>149</sup> and Tb<sup>150</sup> spectra is especially pronounced for two reasons. (a) Tb<sup>151</sup> was more abundantly produced than either Tb<sup>150</sup> or Tb<sup>149</sup>. (b) The measurements were made about 15 hours after the bombardment was over and, while the shorter lived Tb<sup>149</sup> and Tb<sup>150</sup> had decayed through 4 or 5 half-lives, Tb<sup>151</sup> had only decreased to one-half of its original amount. In the Tb<sup>150</sup> spectrum, only the 510- and 640-kev peaks can be assigned to that particular isotope. The 180-, 250-, and 290-kev  $\gamma$  rays are known to belong to Tb<sup>151</sup> from accurate conversion-electron studies.<sup>3</sup> This is also evident from the relative abundance of the three  $\gamma$  rays in the three  $\gamma$ -ray spectra. The 350-kev peak must be assigned to Tb<sup>149</sup> on the basis of the relative  $\gamma$ -ray abundance and, from some recent work by Toth and Rasmussen,<sup>4</sup> it is known that a 350-kev  $\gamma$  ray follows the decay of Tb<sup>149</sup>.

Four decay curves were obtained counting the mass 150 samples "A" and "B" in a flow-type proportional counter and in a single channel scintillation spectrom-

<sup>1</sup> K. O. Nielsen and O. Skilbreid, *Nuclear Instr.* **2**, 15 (1958).

<sup>2</sup> Thompson, Harvey, Choppin, and Seaborg, *J. Am. Chem. Soc.* **76**, 6229 (1954).

<sup>3</sup> Mihelich, Harmatz, and Handley, *Phys. Rev.* **108**, 989 (1957).

<sup>4</sup> K. S. Toth and J. O. Rasmussen, University of California Radiation Laboratory Report UCRL-8375 [*J. Inorg. Nuclear Chem.* **10**, 198 (1959)].